Earth Surface Processes and Landforms
Earth Surf. Process. Landforms **27**, 559–572 (2002)
Published online 19 April 2002 in Wiley InterScience (www.interscience.wiley.com). DOI: 10.1002/esp.331

QUANTIFYING RECENT EROSION AND SEDIMENT DELIVERY USING PROBABILITY SAMPLING: A CASE STUDY

JACK LEWIS*

USDA Forest Service, Pacific Southwest Research Station, Arcata, California 95521, USA

Received 15 January 2001; Revised 14 December 2001; Accepted 19 December 2001

ABSTRACT

Estimates of erosion and sediment delivery have often relied on measurements from locations that were selected to be representative of particular terrain types. Such judgement samples are likely to overestimate or underestimate the mean of the quantity of interest. Probability sampling can eliminate the bias due to sample selection, and it permits the explicit expression of uncertainty with estimates of variance and confidence intervals. In this case study of the Van Duzen River Basin of northwestern California, erosion and sediment delivery originating after 1955 were estimated using a ratio estimator for air-photo-identifiable features greater than 3800 m^3 and a stratified random sample (STRS) of field plots to quantify smaller erosion features. A method is also illustrated for estimating the variance of the ratio of two STRS estimates. Variance estimation permits one to partition the uncertainty associated with different kinds of erosion measurements. The most reliable estimates were obtained from discrete hillslope features, while earthflow yield estimates had extremely high variance. The variance estimates presented can be used to determine sample sizes and allocations required to meet the objectives of future investigations in similar terrain types. Published in 2002 by John Wiley & Sons, Ltd.

KEY WORDS: sediment budgets; erosion; uncertainty; stratified random sampling; ratio estimator

INTRODUCTION

Knowledge of the current sources and quantities of sediment production is needed for many land-management decisions. Managers must understand the relative contributions of different sediment sources in order to evaluate the likely effects of land use and to assign priorities for erosion control. A sediment budget may be constructed to account for the sources and disposition of sediment as it is transported through a watershed (Reid and Dunne, 1996). To estimate erosion and sediment delivery, sediment budgets have often relied on measurements at locations that were selected to be representative of a particular terrain type. Such judgement samples are likely to overestimate or underestimate the mean of the quantity of interest. Bias from selection of the sample can be eliminated through probability sampling. Probability sampling requires that the sample be selected at random and that all sampling units have known probabilities of inclusion in the sample. Accepted sampling design-based estimators of population parameters are either unbiased or nearly so for any population. Additionally, the sampling error can be quantified, permitting confidence intervals to be computed for estimated parameters. Because probability sampling has not been commonly used for estimating erosion, very little is known about the uncertainty in reported erosion estimates. Besides facilitating the construction of confidence intervals, the variance information is also very useful for sample size determination in future investigations. This paper describes the planning, implementation and outcome of a probability sampling design for estimating erosion and sediment delivery, and illustrates the benefits and limitations of the approach.

* Correspondence to: J. Lewis, Redwood Sciences Laboratory, 1700 Bayview Drive, Arcata, California 95521, USA.
E-mail: jlewis01@fs.fed.us

STUDY AREA

The Van Duzen River in California's North Coast Range (Figure 1) is recognized as having been adversely impacted by high sediment loading, and a sediment source investigation was requested by the US Environmental Protection Agency to identify the relative contribution of sediment delivered to stream channels from the various erosional processes which occur on hillslopes and in stream channels throughout the watershed. The Van Duzen River basin drains an area of 1111 km^2, entering the Eel River south of Eureka, California. Elevations range from 19 to 1800 m. A highly active tectonic setting, combined with erodible, unstable terrain and high rainfall rates (125–250 cm between October and April), make the watershed one of the most rapidly eroding in the United States (Brown and Ritter, 1971; Kelsey, 1977). Kelsey estimated a mean sediment yield of 3100 T km ^{2} a ^{1} from the upper half of the basin during 1941–1975. Geologically rapid tectonic uplift and subsequent stream incision have produced a high incidence of landsliding adjacent to stream channels, including large slump-earthflows and, particularly on inner gorge slopes, debris slides. The basin has been classified into five primary terrain types based on bedrock and relative slope stability, as described by Kelsey (1977):

(1) sandstone, generally stable terrain;
(2) sandstone, potentially unstable and active slides;
(3) melange, generally stable, serpentine, and alluvial terrain;
(4) melange, older slump-earthflow terrain;
(5) melange, active slump-earthflow terrain.

Alluvial areas in terrain type 3 include channel migration zones (CMZ), mostly bounded by floodplains and terraces on both banks, where bank erosion is associated with rapid, dramatic shifts in the channel bed.

In addition, the basin has been delineated into three sub-basins, or domains, for comparison purposes. The upper sub-basin is 254 km^2, composed mostly of terrain types 1, 2 and 4, and is managed mainly by the U.S. Forest Service for timber harvesting and recreation. The middle sub-basin is 523 km^2, composed mostly of terrain types 4 and 5, with some of types 1 and 2, and is managed primarily for livestock production and

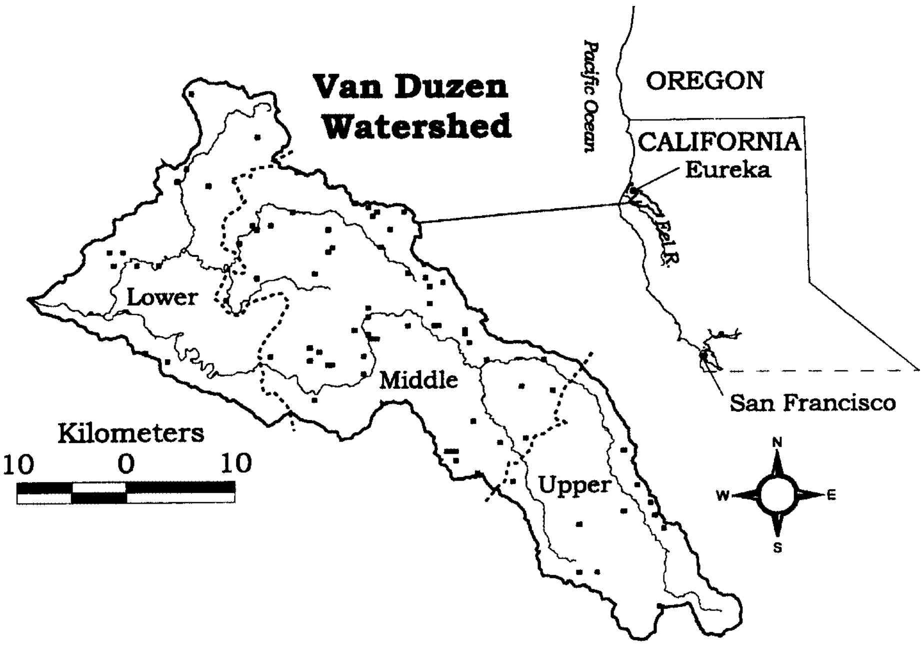

Figure 1. Van Duzen watershed location map showing the 80 sampled plots in the upper, middle and lower sub-basins

sporadic timber harvesting. The lower sub-basin is 334 km^2, dominated by terrain types 1, 2 and 3, and is managed primarily for timber production by large industrial landowners.

METHODS

Erosion and sediment delivery originating after 1955 were estimated with a complete inventory of air-photo-identifiable features with void volumes greater than 3800 m^3 and a stratified random sample (STRS) of field plots to quantify smaller erosion features. Air photos going back to 1955 helped establish the ages of large features, and vegetation was the primary age indicator on field plots. Photo-identified features encountered en route to field plots served as ground truth to correct photo-estimated erosion volumes.

STRS plot measurements included erosional voids measuring greater than 7·6 m^3 in volume, excluding those identified in the air-photo inventory, and earthflows. Thus minor surface erosion (e.g. rainsplash, sheet and rill erosion) and creep were not quantified. Estimates of surface erosion rates from the neighbouring South Fork Eel River and Redwood Creek suggested that surface erosion and soil creep would account for no more than 10 per cent of the annual basin sediment delivery (US Environmental Protection Agency, 1999; Stillwater Sciences, 1999). Void volumes were estimated as the product of the mean width, depth and length of features. Sediment delivery was estimated as the volume delivered to a stream channel, determined by tracing the sediment's transport path and surveying the deposits. Any apparent land use or management associations were also recorded with the objective of quantifying the portion of sediment that might be controllable.

Erosion features were characterized in the field as: shallow debris slides; shallow debris slides which triggered channelized debris flows or torrents; scoured debris torrent tracks, large and small earthflows; road, skid trail or hillslope gullies; streambank erosion; or channel erosion. These categories were lumped into earthflow and non-earthflow features for this analysis. STRS estimates of earthflow and non-earthflow sources are separated because of the much greater uncertainty in quantifying sediment originating from earthflows. Earthflow erosion and sediment delivery were difficult to quantify because estimating movement rates, topographic deflation rates, and the depth to the basal slip surface or failure plane can be highly error-prone and depended partly on indirect information from published reports (Kelsey, 1977, 1980; Iverson, 1984; Nolan and Janda, 1995; Swanston *et al*., 1995).

Channel migration zones

Two prominent CMZs are found in the watershed: a 26-km reach in the lower sub-basin, and a 14-km reach in the middle and upper sub-basins. During the conduct of the investigation, it became apparent that contributions of sediment from these areas had to be quantified separately from the plot and photo estimates. The need arose because: (1) erosion and yield estimates from the stable melange, terrain type 3, would be greatly exaggerated if the sample plots included large sums of erosion associated with bank erosion in the CMZs; (2) the estimation of volumes was much less certain than for landslides, gullies and other more discrete sources; and (3) estimating large alluvial sediment sources required a different set of methods. CMZ source areas were inventoried by mapping and interpreting channel changes that occurred between the 1941 and 1997 aerial photographs. Depths were estimated separately for eroded terraces, floodplains and stabilized gravel bars. The sediment contribution from CMZs was not estimated statistically and is included here for completeness only.

Planning

A complete erosion inventory was available from Jordan Creek, a nearby tributary of the lower Eel River that is geologically similar to terrain type 2 in the Van Duzen basin (Pacific Watershed Associates, 1999). An 18·75-ha grid was overlaid onto the erosion map and the 67 grid squares were aggregated into all possible plots of 1 × 1, 1 × 2, 2 × 2, 3 × 3 and 4 × 4 grid squares. For each plot size, an analysis of variance (ANOVA) was performed on groups of non-overlapping plots. The ANOVA mean squares within groups (MS_w) provided estimates of the variance between plots of each size. These were converted to standard errors for the per-hectare erosion rate based on the five plot sizes (18·75 to 300 ha) using:

$$s = \frac{\sqrt{MS_w}}{area} \tag{1}$$

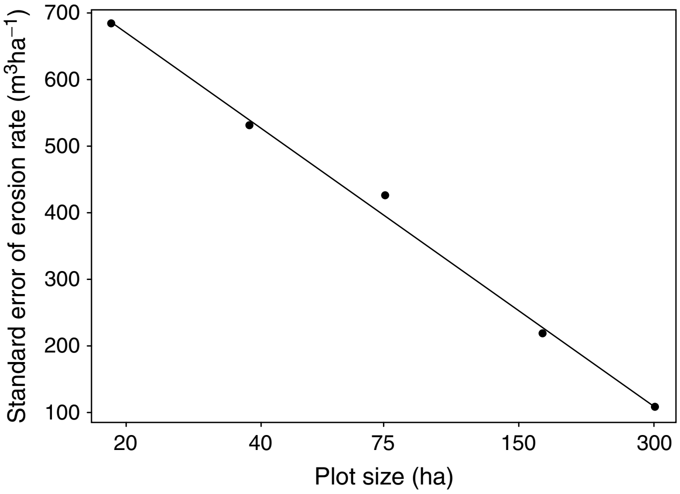

Figure 2. Variability among plots in nearby Jordan Creek (terrain type 2) decreases with increasing plot size. Scale of x-axis is logarithmic

As expected, the estimated erosion rate becomes more reliable as plot size increases. The standard error of the erosion rate was found to vary linearly with the logarithm of plot size (Figure 2) as described by the relation:

$$s = 1291 \quad 207\ \ln(area) \tag{2}$$

A similar relation was developed excluding photo-identifiable features greater than 3800 m^3. These relations can be used to determine the sample size needed to estimate erosion in terrain type 2 with any desired precision for various plot sizes.

In a stratified design, one first needs to consider the optimal allocation of plots to strata. Lacking information about variability in the other terrain types, we assumed that the coefficient of variation among plots would be equal in each terrain type. If the costs of travelling between and measuring plots are to be considered then the optimal allocation under the above assumption is:

$$w_h = \frac{T_h / c_h^{0\cdot5}}{\sum_h T_h / c_h^{0\cdot5}} \tag{3}$$

where, in stratum h, w_h is the proportion of all sample plots allocated to the stratum, T_h is the total erosion, and c_h is the cost of travel and measurement per plot. We found that the variability among T_h was much greater than that among c_h, so assumptions about costs had very little influence on the allocation compared to assumptions about T_h. Assuming that the costs of measurement and travel are the same in all strata leads to the result that the number of plots in each stratum should be proportional to T_h. Preliminary estimates of erosion rates in each stratum were available from a previous study that had been conducted in the upper two-thirds of the watershed (Kelsey, 1977). Knowing the areas in each terrain type then permitted us to estimate each T_h.

The 'optimal' allocation, based on the single objective of minimizing the variance of the estimated total erosion, would have put most of the sampling effort in strata 2, 4 and 5, providing very little information about the two more stable strata (Table I). In order to provide a minimum of information about terrain types 1 and 3, and to protect against the possibilities that (1) preliminary erosion rates were incorrect, and (2) that the strata defined by regular-shaped field plots would contain inclusions of unintended terrain types, the

Table I. Stratum areas, inclusions, and allocation of sample to strata

Stratum	Area (km^2)	Inclusions (%)	Fraction of basin (%)	Optimal allocation (%)	Chosen allocation (%)	Fraction sampled (%)
1	538	11·6	48·4	1·2	10·0	0·25
2	114	21·3	10·3	40·0	31·3	3·70
3	117	18·2	10·5	3·3	5·0	0·58
4	315	14·8	28·4	29·8	31·2	1·34
5	27	28·9	2·4	25·7	22·5	11·25
Total	1111	14·6	100·0	100·0	100·0	1·22

allocation was increased from 1·2 to 10 per cent in stratum 1 (the largest stratum), and from 3·3 to 5 per cent in stratum 2.

We assumed it would be too expensive to measure all erosion on plots of the size being considered, so our original design included multi-stage sampling of nested plots within each stratum. Only features greater than 380 m^3 were to be measured in the first-stage plots. A smaller second-stage plot would be selected at random within each selected first-stage plot for measurement of features greater than 76 m^3. And a still smaller third-stage plot would be selected at random within each selected second-stage plot for measurement of features greater than 7·6 m^3.

To determine the best configuration of plot sizes, relations such as Equation (2) were developed from the Jordan Creek data for each of the erosion size classes, excluding photo-identifiable features greater than 3800 m^3. Then a table was built showing the expected variance and cost of various combinations of plot sizes and sample sizes, all conforming to the chosen allocation shown in Table I. For any fixed cost, the combination of plot sizes giving the lowest variance was then identified. This procedure led to the decision that first-stage sampling units should contain nine equal size second-stage units, which in turn would contain nine equal size third-stage units. Exactly one second-stage unit and one third-stage unit would be sampled in each plot. The smallest unit was set at 0·209 ha, fixing first-stage plots at 16·9 ha. A sample size of 80 such plots was expected to provide a coefficient of variation (defined here as the ratio of the standard error to the estimated total) of 0·16.

Once field work began, it was found that the time spent to traverse and map the sample plot consumed most of the time, and measuring all erosion greater than 7·6 m^3 did not appreciably increase the time on the plot. Consequently, the strategy was modified to map all erosional features within the 16·9-ha plots and not differentiate the erosion into the three volume classes. This decision was also expected to improve estimation by eliminating sampling variance introduced by the second and third stages of subsampling.

Plot selection

A 16·9-ha grid was developed for the entire basin using a GIS. Grid cells on the watershed boundary were included only if at least half their area lay within the basin. A terrain type coverage was overlaid upon the grid and cells were assigned to strata according to their dominant terrain-type. On average, 85 per cent of the area in a sampled cell belonged to its assigned type. The erosion and delivery estimates reported for individual strata therefore reflect inclusions (Table I) due to representation of geologic types with a coarse grid.

A list of 200 random cells was generated and landowner permission for access was sought for 80 cells on the list: the first eight cells within geology stratum type 1, the first 25 in stratum type 2, the first four in stratum type 3, the first 25 in stratum type 4 and the first 18 in stratum type 5. When landowner permission could not be obtained, the next cell on the list for the appropriate stratum was selected. The 80 cells obtained in this manner served as the field sample.

Estimation of totals

Total erosion and delivery were estimated according to standard formulas (e.g. Cochran, 1977) for stratified random sampling:

$$\widehat{T} = \sum_{h=1}^{L} \widehat{T}_h = \sum_{h=1}^{L} N_h \bar{y}_h = \sum_{h=1}^{L} N_h \sum_{i=1}^{n_h} \frac{y_{hi}}{n_h} \tag{4}$$

where $\widehat{T}$ = estimated total erosion or sediment delivery, $\widehat{T}_h$ = estimated total in stratum h, L = total number of strata, N_h = total number of grid cells in stratum h, n_h = number of sampled grid cells in stratum h, y_{hi} = erosion or sediment delivery in ith sampled cell of stratum h and $\bar{y}_h$ = estimated mean erosion or sediment delivery in stratum h.

Variances and standard errors were computed as follows:

$$\widehat{V}(\widehat{T}) = \sum_{h=1}^{L} \widehat{V}(\widehat{T}_h) = \sum_{h=1}^{L} N_h^2 \widehat{V}(\bar{y}_h) = \sum_{h=1}^{L} N_h^2 \frac{N_h \quad n_h}{N_h} \frac{s_h^2}{n_h} \tag{5}$$

where $\widehat{V}(\cdot)$ = estimated variance of the quantity in parentheses, and

$$s_h^2 = \sum_{i=1}^{n_h} \frac{(y_{hi} - \bar{y}_h)^2}{n_h \quad 1} \tag{6}$$

In addition, totals were requested for the upper, middle and lower watershed. These sub-basins, or domains, were of interest because of physiographic and management differences. Sub-basin results were computed with Equations 4 to 6, treating sub-basins as populations, with the following exception. Because the sampling design did not stratify by sub-basins, the upper and lower sub-basins by chance contained less than two plots in some of the strata. Variance estimation is not possible in such circumstances, and estimation of a mean from a single plot is undesirable. Therefore, when a stratum contained zero or one plot in a sub-basin, the sub-basin erosion and delivery rates and corresponding variances were assumed to be the same as those for the stratum as a whole, i.e. $\bar{y}_h$ and $\widehat{V}(\bar{y}_h)$ for the whole basin were substituted for those of the sub-basin.

Air photo analysis

Large features equalling or exceeding 3800 m^3 in volume were identified using aerial photographs from 1955, 1966, 1974, 1984, 1990, 1994 and 1997. Features of that size could be reliably identified on the variety of available photography, which varied in scale from 1:12 000 to 1:40 200 and included black-and-white, colour and infrared films. If a previously identified erosional feature showed obvious enlargement between photo periods, the new volume of erosion was added to the original feature. The volume of features was estimated by multiplying their area on the photo by their estimated mean depth. Depths were estimated using a regression of depths from field-verified features versus photo areas. While travelling to the STRS field plots, 56 of the photo-identified features were field-verified and measured in detail. The correlation between field and photo-estimated volumes was 0·67 (Figure 3). A ratio estimator (e.g. Cochran, 1977) was used to estimate the total erosion from photo-identified features:

$$\hat{T}_p = \hat{R}_p T_x = \frac{\bar{y}}{\bar{x}} T_x \tag{7}$$

where $\widehat{T}_p$ = estimated total erosion from photo-identified features, $\widehat{R}_p$ = sample ratio of field-estimated to photo-estimated volumes, T_x = total of all photo-estimated volumes, $\bar{y}$ = sample mean of field-estimated volumes and $\bar{x}$ = sample mean of photo-estimated volumes that were field-verified.

The ratio $\widehat{R}_p$ is the slope of a weighted least squares regression line through the origin, with weights inversely proportional to x. The estimated ratio $\widehat{R}_p = 0{\cdot}989$ suggests the photo-estimated volumes are not systematically

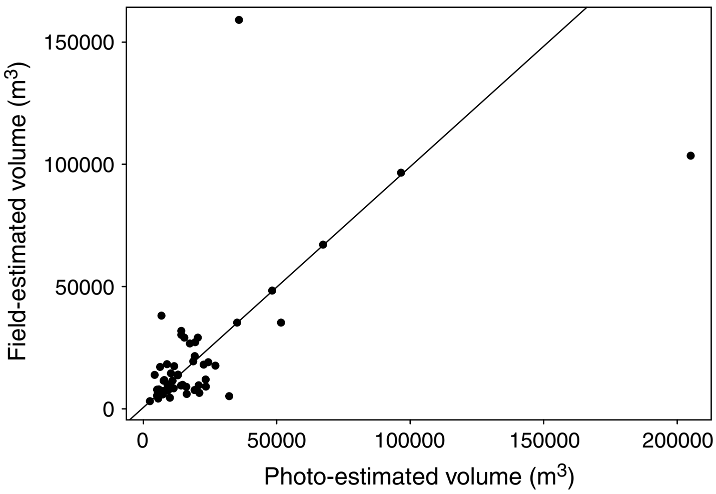

Figure 3. Scatterplot of field-estimated versus photo-estimated erosion volumes. Slope of weighted least squares regression line is the ratio estimator $\hat{R}_p = 0{\cdot}989$

biased. If the two outliers in Figure 3 are omitted, the ratio changes to 0·963, still not far from 1. The outliers were retained because they are needed to properly characterize the variance. The traditional variance estimator, based on a simple random sample of field-verified features is given by:

$$\widehat{V}(\widehat{T}_p) = \frac{N(N-n)}{n(n-1)} \sum_{i=1}^{n} (y_i - \widehat{R}_p x_i)^2 \tag{8}$$

where N = number of photo-identified features in population, n = number of photo-identified features that were measured in field, y_i = ith field-estimated volume in sample and x_i = photo-estimated volume corresponding to y_i.

To estimate volumes for domains (in this case sub-basins or STRS strata) we chose to use an estimate of $\widehat{R}_p$ based on the entire sample, because we did not expect the ratio to vary among domains. Thus domain estimates of the total were simply estimated as:

$$\widehat{T}_d = T_{xd}\widehat{R}_p \tag{9}$$

where $\widehat{T}_d$ = estimated volume of photo-identified features in domain d and T_{xd} = total of all photo-estimated volumes in domain d.

The variance estimator (Equation 8) tends to give high values with samples having high values of $\bar{x}$ and low values with samples having low values of $\bar{x}$ (Thompson, 1992). In our sample, the mean was 45 per cent higher than the population mean. We therefore employed an alternative variance estimator for $\widehat{T}_p$ that is unbiased if the data obey a model in which (1) the relation between y_i and x_i is a straight line through the origin, (2) the variance of y_i about this line is proportional to x_i, and (3) the errors are uncorrelated. This estimator is model-unbiased, i.e. unbiased with respect to the modelled distribution of y, in contrast to design-unbiased estimators, such as Equation 5, which are unbiased with respect to the distribution of y over all possible samples. See Gregoire (1998) for a discussion of these concepts. Random sampling is not a requirement for model-unbiasedness. The alternative estimator is also robust to departures in the variance assumption (Thompson, 1992; Royall and Cumberland, 1981). The robust estimator is given by:

$$\widehat{V}_R(\widehat{T}_p) = \frac{\mu_x \bar{x}_{\bar{s}} \widehat{V}(\widehat{T}_p)}{\bar{x}_s^2(1 - V^2/n)} \tag{10}$$

where μ_x = mean of all photo-estimated volumes, $\bar{x}_s$ = mean of photo-estimated volumes for features that were measured in the field and $\bar{x}_{\not s}$ = mean of photo-estimated volumes for features *not* measured in the field, and

$$V = \frac{\sum_{i=1}^{n}(x_i - \bar{x}_s)^2}{(n \quad 1)\bar{x}_s^2} \tag{11}$$

Potential controllability

Erosional features were classified as potentially controllable if there was more than minor evidence that the land use activity could have contributed to the erosion. Included were erosional features in any kind of clearcut harvest, partial or selection harvest, road, skid trail, grazing or homesteading and land development activities. Most non-earthflow sediment sources on intensively managed areas outside of the CMZ were considered to be controllable for this analysis. The proportion of controllable erosion (or sediment yield) was estimated as the ratio of the STRS estimates of controllable volume, $\widehat{T}_y$, and total volume, $\widehat{T}_z = \widehat{T}$:

$$\widehat{R}_{yz} = \widehat{T}_y / \widehat{T}_z \tag{12}$$

$\widehat{R}_{yz}$ is sometimes called a 'combined ratio' because a single ratio is estimated for all strata (Cochran, 1977; Särndal *et al.*, 1992). Its variance is estimated by:

$$\widehat{V}(\widehat{R}_{yz}) = \frac{1}{\hat{T}_z^2} \sum_{h=1}^{L} \frac{N_h(N_h \quad n_h)}{n_h(n_h \quad 1)} \sum_{i=1}^{n_h} (e_{hi} - \bar{e}_h)^2 \tag{13}$$

in which $e_{hi} = y_{hi} \quad \widehat{R}_{yz} z_{hi}$ and $\bar{e}_h = \sum_{i=1}^{n_h} e_{hi}$.

The proportion of controllable photo-identifiable erosion (or sediment yield) was computed as the ratio of the photo-identifiable controllable volume, $\widehat{T}_{py}$, and photo-identifiable total volume, $\hat{T}_{pz} = \hat{T}_p$:

$$\widehat{R}_{pyz} = \widehat{T}_{py} / \widehat{T}_{pz} = T_{xy} \widehat{R}_p / T_{xz} \widehat{R}_p = T_{xy} / T_{xz} \tag{14}$$

where T_{xy} and T_{xz} are the photo-estimated volumes of controllable and total erosion, respectively. Note that, since $\widehat{R}_p$ dropped out of the calculation, $\widehat{R}_{pyz}$ is not actually a random variable and no variance estimate is possible.

Confidence intervals and coefficients of variation

Approximate 95 per cent confidence intervals are conventionally reported as $\hat{\theta} \pm 1{\cdot}96\sqrt{\widehat{V}(\hat{\theta})}$, where $\widehat{\theta}$ represents the quantity being estimated (e.g. $\widehat{T}, \widehat{T}_p$ or $\widehat{R}_{yz}$). For ease of interpretation, we instead report the estimated coefficient of variation:

$$CV = \frac{\sqrt{\hat{V}(\hat{\theta})}}{\hat{\theta}} \tag{15}$$

For the estimator $\hat{T}_d$ the estimated coefficient of variation, CV_d, is identical to that for $\widehat{T}_p$ (CV_p) because, from Equations 7 and 9, we have:

$$V(\widehat{T}_p) = T_x^2 V(\widehat{R}_p) \tag{16}$$

$$V(\widehat{T}_d) = T_{xd}^2 V(\widehat{R}_p) = \frac{T_{xd}^2}{T_x^2} V(\widehat{T}_p) \tag{17}$$

and, letting

$$\widehat{V}(\widehat{T}_d) = \frac{T_{xd}^2}{T_x^2}\widehat{V}(\widehat{T}_p) \tag{18}$$

it follows that

$$CV_d = \frac{\sqrt{\widehat{V}(\widehat{T}_d)}}{\widehat{T}_d} = \frac{T_{xd}\sqrt{\widehat{V}(\widehat{T}_p)}\ /\ T_x}{T_{xd}\widehat{R}_p} = \frac{\sqrt{\widehat{V}(\widehat{T}_p)}}{\widehat{T}_p} = CV_p \tag{19}$$

RESULTS

Tables II and III show erosion and sediment delivery, including stratum estimates. Estimates of totals have been converted to erosion and delivery rates over the 44-year period using $\widehat{Y} = \widehat{T}/44A$, where A represents the area of the pertinent population, stratum, or domain, after removing any CMZ areas. Since photo-identified features were not a stratified random sample, estimates for photo-identified features treat strata as domains, utilizing Equations 9 and 19.

Erosion and delivery rates from earthflows were very similar in the active and older slump-earthflow terrain types (4 and 5), but rates from non-earthflow features were higher in the active slump-earthflow terrain. Nevertheless, the older slump-earthflow terrain contributed greater volumes of sediment because of its greater area. As expected, the highest non-earthflow erosion rates were from terrain type 2 (sandstone, potentially unstable and active slides). The stable terrain types, 1 and 3, had the lowest erosion rates.

Coefficients of variation for total non-earthflow erosion and sediment delivery were 0·21 and 0·17, respectively, much lower than the corresponding values, 0·49 and 0·73, for earthflows (Tables II and III). Because they are based on smaller sample sizes, estimates of individual stratum totals and rates generally have larger

Table II. Erosion by stratum ($m^3 km^{-2} a^{-1}$): non-earthflow (non-EF), earthflow, plot total = non-EF + earthflow, and photo-identifiable (photo-ID)

Terrain type	N	n	Non-EF		Earthflow		Plot total		Photo-ID	
			$\hat{Y}$	CV	$\hat{Y}$	CV	$\hat{Y}$	CV	$\hat{Y}$	CV
1	3180	8	90	0·70	0	0·00	90	0·47	46	0·15
2	675	25	643	0·23	146	0·86	789	0·30	1144	0·15
3	690	4	47	0·70	126	1·00	173	0·68	36	0·15
4	1860	25	197	0·27	904	0·59	1100	0·48	54	0·15
5	160	18	392	0·34	1049	0·42	1441	0·31	561	0·15
Total	6565	80	182	0·21	313	0·49	495	0·32	174	0·15

Table III. Sediment delivery by stratum ($m^3 km^{-2} a^{-1}$): non-earthflow (non-EF), earthflow, plot total = non-EF + earthflow, and photo-identifiable (photo-ID)

Terrain type	N	n	Non-EF		Earthflow		Plot total		Photo-ID	
			$\hat{Y}$	CV	$\hat{Y}$	CV	$\hat{Y}$	CV	$\hat{Y}$	CV
1	3180	8	32	0·44	0	0·00	32	0·52	25	0·14
2	675	25	472	0·28	26	0·91	498	0·29	762	0·14
3	690	4	24	0·84	13	1·00	37	0·54	30	0·14
4	1860	25	151	0·31	514	0·82	664	0·64	33	0·14
5	160	18	358	0·37	539	0·69	896	0·43	263	0·14
Total	6565	80	119	0·17	165	0·73	285	0·44	111	0·14

Table IV. Erosion by sub-basin ($m^3 km^{-2} a^{-1}$): non-earthflow (non-EF), earthflow, plot total = non-EF + earthflow, and photo-identifiable (photo-ID)

Sub-basin	N	n	Non-EF		Earthflow		Plot total		Photo-ID	
			$\hat{Y}$	CV	$\hat{Y}$	CV	$\hat{Y}$	CV	$\hat{Y}$	CV
Upper	1502	11	304	0·35	19	0·64	323	0·32	184	0·15
Middle	3090	56	198	0·19	555	0·50	753	0·37	173	0·15
Lower	1973	13	165	0·38	103	0·49	268	0·30	169	0·15
Total	6565	80	182	0·21	313	0·49	495	0·32	174	0·15

Table V. Sediment delivery by sub-basin ($m^3 km^{-2} a^{-1}$): non-earthflow (non-EF), earthflow, plot total = non-EF + earthflow, and photo-identifiable (photo-ID)

Sub-basin	N	n	Non-EF		Earthflow		Plot total		Photo-ID	
			$\hat{Y}$	CV	$\hat{Y}$	CV	$\hat{Y}$	CV	$\hat{Y}$	CV
Upper	1502	11	253	0·41	3	0·52	257	0·41	122	0·14
Middle	3090	56	138	0·22	300	0·73	438	0·51	112	0·14
Lower	1973	13	61	0·36	49	0·78	109	0·40	99	0·14
Total	6565	80	119	0·17	165	0·73	285	0·44	111	0·14

coefficients of variation than estimates of population totals. Because of the chosen stratum allocations, the greatest relative uncertainty is appropriately associated with the terrain types that contribute the least sediment.

The greatest erosion and delivery rates are from the middle sub-basin (Tables IV and V), primarily because of its high input from earthflows. The upper sub-basin apparently contributes the most sediment from non-earthflow features, because it has a larger proportion of stratum 2 and because erosion and delivery rates from stratum 2 are highest in the upper sub-basin. However, the differences in erosion and delivery rates between the sub-basins are not statistically significant, perhaps because only three plots from stratum 2 were located in the upper sub-basin.

As measured by *CV*, uncertainty for both non-earthflow erosion and delivery rates was greater in the upper and lower basins, because they contained only 14 per cent and 16 per cent of the total sample, respectively. These percentages reflect their sizes and terrain type compositions as well as an element of chance. The middle sub-basin is the largest of the three, and only 43 per cent of it is contained in the two sparsely sampled stable terrain types, compared with 61 per cent of the upper sub-basin, and 82 per cent of the lower sub-basin. Most of the earthflow erosion and sediment delivery originates in the middle sub-basin, but there is a great deal of uncertainty in the exact rates because of its tremendous variability.

In the basin as a whole, photo-identified features greater than 3800 m^3 accounted for similar but slightly smaller amounts of erosion and sediment delivery than smaller non-earthflow features estimated from the randomly located plots (Tables II and III). The large photo-identified features were concentrated in the unstable sandstone terrain type and, to a somewhat lesser degree, in the mélange, active slump-earthflow terrain.

Bank erosion in the 18 km^2 CMZ area was estimated at 115 000 $m^3 a^{-1}$, contributing about 21 per cent of the sediment delivered to the channel in the 44 year period. Of this amount 86 per cent originated from terraces and floodplains. Since these estimates were not based on a sample or a statistical model, we have no associated measure of uncertainty.

In the whole basin, an estimated 37 per cent of the sediment delivery from non-earthflow sources, 5 per cent of that from earthflow sources, and 40 per cent of the large (>3800 m^3) sources was judged potentially controllable (Table VI). Percentages from the lower basin were higher than from the upper and middle basins, reflecting the prevalence of industrial timberlands in the lower basin. In the lower basin, an estimated 63 per

Table VI. Potential controllable percentage of sediment delivery by sub-basin: non-earthflow (non-EF), earthflow, plot total = non-EF + earthflow, and photo-identifiable (photo-ID)

Sub-basin	N	n	Non-EF		Earthflow		Plot total		Photo-ID	
			$\hat{R}_{yz}$	CV	$\hat{R}_{yz}$	CV	$\hat{R}_{yz}$	CV	$\hat{R}_{pyz}$	CV
Upper	1502	11	22	0·68	0	–	22	0·67	30	–
Middle	3090	56	28	0·22	5	0·18	13	0·34	29	–
Lower	1973	13	91	0·05	1	0·00	44	0·39	63	–
Total	6565	80	37	0·20	5	0·17	19	0·35	40	–

cent of the large sources and 91 per cent of all non-earthflow sources, but none of the earthflow sources, were judged controllable.

DISCUSSION

This study illustrates how sources of uncertainty can be identified and partitioned when quantifying sediment source volumes using probability sampling. It became clear, for example, that discrete, non-earthflow, sources can be quantified reasonably well using an STRS approach and the variance results can serve as a guide to plan future sampling designs in similar terrain types. On the other hand, earthflow sources have much greater uncertainty and would require much greater sample sizes to yield reasonable confidence intervals. However, if the influence of land management on earthflows is relatively limited, the expense of such efforts may not be warranted for many practical purposes.

The coefficients of variation for photo-identified sediment sources indicate that this method produces quite reliable estimates for large features. The reliability stems from the efficiency of the ratio estimator, which utilizes auxiliary information (photo-estimated volumes) on the entire population together with a weighted regression comparing the auxiliary information to the target variable. Despite its wide scatter, the relationship (Figure 3) between photo-estimated volumes and field measurements of the same features apparently was adequate to provide reasonable limits on the uncertainty of the estimated total.

Estimation for sub-basins could have been improved if they had been included as a second level of stratification in the sampling design, instead of treating them as domains with random sample sizes. Stratifying on sub-basins would have permitted us to set the sample sizes in each sub-basin and terrain type to ensure that adequate information would be obtained from each. However, to achieve reasonable confidence limits on each sub-basin would have required more than the 80 plots this project budgeted for.

Allocation of plots to strata

The sampling design was based partly on an objective of achieving a coefficient of variation of 0·16 for erosion in the whole basin. This was achieved for photo-identified sources ($CV = 0{\cdot}15$ for erosion and 0·14 for delivery) and nearly achieved for non-earthflow features ($CV = 0{\cdot}21$ for erosion and 0·17 for delivery), but not for earthflow sources ($CV = 0{\cdot}49$ for erosion and 0·73 for delivery). Such a result might have been anticipated because Jordan Creek, the watershed from which initial variance estimates were obtained, does not contain any earthflow terrain. For lack of better information, we assumed that the coefficient of variation among plots (CVP) was the same in all terrain types. Under that assumption, the optimal allocation of sample plots to strata was proportional to the stratum totals. Having now collected the data, we can check that assumption.

The *CVP* of non-photo-identifiable erosion on 18·6-ha plots at Jordan Creek was 1·08, quite similar to the value of 1·15 (Table VII) estimated from the sample of 16·9-ha plots on the same terrain type (stratum 2) in the Van Duzen basin. In addition, the mean erosion rates differed by only 8 per cent. For non-earthflow delivery, the *CVP* averages close to 1·50 and does not vary much between strata (Table VII). It appears to vary somewhat more for non-earthflow erosion than for delivery. For earthflows (both erosion and delivery), the *CVP* is greater and much more variable than for non-earthflow sources.

Table VII. Analysis of sample allocation for estimating the total of various responses

Response	Terrain Type	Total ($10^6 m^3$)	% of total	N_h	s_h (m^3)	*CVP*	Optimal allocation	Actual allocation
	1	2·13	24·3	3180	1320	1·97	33·3	10·0
Non-EF	2	3·22	36·8	675	5506	1·15	29·5	31·2
erosion	3	0·20	2·3	690	412	1·41	2·3	5·0
	4	2·72	31·2	1860	2006	1·37	29·6	31·2
	5	0·47	5·4	160	4166	1·42	5·3	22·5
	1	0·76	13·2	3180	299	1·25	11·5	10·0
Non-EF	2	2·36	41·2	675	4878	1·39	39·7	31·2
sediment	3	0·11	3·2	690	256	1·67	2·1	5·0
delivery	4	2·09	29·8	1860	1719	1·53	38·6	31·2
	5	0·43	25·7	160	4147	1·55	8·0	22·5
	1	0·00	0·0	3180	0	–	0·0	10·0
Earthflow	2	0·73	4·9	675	4684	4·30	7·3	31·2
erosion	3	0·55	3·6	690	1583	1·99	2·5	5·0
	4	12·51	83·1	1860	19 706	2·93	84·9	31·2
	5	1·25	8·3	160	14 083	1·79	5·2	22·5
	1	0·00	0·0	3180	0	–	0·0	10·0
Earthflow	2	0·13	1·6	675	886	4·56	1·9	31·2
sediment	3	0·05	0·7	690	158	1·99	0·3	5·0
delivery	4	7·11	89·5	1860	15 592	4·07	91·8	31·2
	5	0·64	8·1	160	11 698	2·91	5·9	22·5

Assuming equal costs per stratum, optimal allocations are proportional to $N_h s_h$, as shown in Table VII. The allocation used was a good allocation for non-earthflow yield, and not too bad for non-earthflow erosion (Table VII). For the latter, some of the sampling effort in stratum 5 would apparently have been better spent in stratum 1. For earthflow erosion and yield, clearly most of the effort needed to be in stratum 4. Because of the larger yields and higher variability of earthflows compared to non-earthflows, optimal allocations for total erosion or yield (excluding photo-identified features greater than 3800 m^3) would also focus most sampling in stratum 4, with stratum 2 a fairly distant second priority. However, as stated earlier, it may be unwise to place the great majority of effort in a single terrain type in which the erosion may be uncontrollable as well as being very difficult to measure reliably. This is particularly true if such effort would be at the expense of information from other terrain types whose properties may not be well studied.

Sources of error

The variance estimates for the STRS estimators $\widehat{T}$ and $\widehat{R}_{yz}$ include variation due to sampling, sampling design and measurement.

1. *Sampling*. Estimates are based on a sample from the population, only one of many possible samples that could have been selected under the given design.
2. *Measurement*. Repeated measurements of the same feature, by the same or different observers, are unlikely to be identical. Erosion volumes were approximated by a mean width, length and depth. Depth can only be determined by guessing at the height of the original land surface. Estimation of creep and topographic deflation rates for earthflow sediment delivery, determination of whether a feature originated after 1955, and estimation of the proportion of erosion that reached a stream channel are all inexact procedures.
3. *Design inefficiencies*. Stratum inhomogeneities caused by inaccurately mapped terrain types or their representation as a grid result in increased variance relative to a design in which strata do not contain inclusions of other types.

The variance estimates for photo-estimated erosion, $\widehat{T}_p$, are a function of the residual variance in Figure 3, which reflects the measurement variance in both field-estimated and photo-estimated volumes.

There are also a number of sources of error not reflected in the variance estimates.

1. *Measurement bias*. Systematic measurement errors might include, for example, a tendency to underestimate or overestimate creep rates. Any of the sources of measurement variance mentioned above could also be sources of measurement bias.
2. *Non-response*. Some landowners could not be contacted or refused access to their land.
3. *Unmeasured features*. Some older revegetated features may not have been identified. To reduce costs, surface erosion on bare soil and features smaller than 7·6 m^3 were deliberately not measured.
4. *Features estimated non-statistically*. For reasons mentioned earlier, erosion and sediment delivery from banks in the CMZ were excluded from the sampling protocols and estimated non-statistically utilizing a combination of sequential aerial photographs and bank height measurements.

CONCLUSIONS

Sediment source volumes from an 1111-km^2 catchment were quantified by partitioning the sediment sources into two size classes, using a ratio estimator for large photo-identifiable sources, and using stratified random sampling of field plots to estimate the contribution from smaller sources. Both of these methods were effective on features whose volumes could be reliably measured from voids remaining on hillslopes. However, the variance estimates confirmed that there is tremendous uncertainty in estimating sediment contributions from earthflows.

Estimation of sub-basin sources would have been improved if the design had incorporated stratification by sub-basin as well as by terrain type. However, reliable estimation for sub-populations and strata generally will require larger sample sizes.

Ratios between contributions from different sediment source types can be statistically quantified using the combined ratio estimator and its associated variance estimator. In this investigation, these were used to estimate the ratio of preventable erosion to total erosion.

Statistical variance estimates include variability due to sampling, imprecise measurement, and inherent design limitations. However, they do not include errors due to measurement bias or the inability to access or identify certain parts of the population. Certain errors may also be deliberately introduced or ignored to control costs.

The chief benefits of the probability sampling approach are that it provides (1) design-unbiased estimation of totals, (2) explicit treatment of uncertainty, and (3) variance estimates that can be used to determine sample sizes and allocations required to meet the objectives of future investigations.

ACKNOWLEDGEMENTS

This project was funded by the US Environmental Protection Agency and carried out under contract with Pacific Watershed Associates, PO Box 4433, Arcata, CA, who prepared a final report in November 1999, entitled ‘Sediment Source Investigation for the Van Duzen River Watershed’. Danny Hagans of PWA managed the project and directed fieldwork. Cooperation and assistance from numerous landowners and land managers were necessary to complete the fieldwork. These included the Pacific Lumber Company, Sierra Pacific Industries, Simpson Timber Company, Six Rivers National Forest, and the Yager/Van Duzen Environmental Stewards organization.

REFERENCES

Brown WM III, Ritter JR. 1971. *Sediment transport and turbidity in the Eel river basin*. US Geological Survey Water Supply Paper, No. 1986.

Cochran WG. 1977. *Sampling Techniques*, (3rd edn.). John Wiley: New York.

Gregoire TG. 1998. Design-based and model-based inference in survey sampling: appreciating the difference. *Canadian Journal of Forestry Research* **28**: 1429–1447.

Iverson RM. 1984. *Unsteady, nonuniform landslide motion: theory and measurement*. PhD Thesis, Stanford University, California.

Kelsey HM. 1977. *Landsliding, channel changes, sediment yield and land use in the Van Duzen River basin, north coastal California, 1941–1975*. PhD Thesis, University of California, Santa Cruz.
Kelsey HM. 1980. A sediment budget and an analysis of geomorphic process in the Van Duzen River basin, California, 1941 to 1975. *Geological Society of America Bulletin* **91**: 190–195, 1119–1216.
Nolan KM, Janda RJ. 1995. Movement and sediment yield of two earthflows, northwestern California, In: *Geomorphic Processes and Aquatic Habitat in the Redwood Creek Basin, Northwestern California*. F1–F12 US Geological Survey Professional Paper, No. 1454.
Pacific Watershed Associates. 1999. *Sediment source investigation and sediment reduction plan for the Jordan Creek watershed, Humboldt County, California*.
Reid LM, Dunne T. 1996. *Rapid Evaluation of Sediment Budgets*. Catena Verlag: Reiskirchen, Germany.
Royall RM, Cumberland WG. 1981. An empirical study of the ratio estimator and estimators of its variance. *Journal of the American Statistical Association* **76**(373): 66–77.
Särndal C, Swensson B, Wretman J. 1992. *Model Assisted Survey Sampling*. Springer-Verlag: New York.
Stillwater Sciences. 1999. *South Fork Eel TMDL: Sediment source analysis*. Report prepared for Tetra Tech, Inc., Fairfax, Virginia.
Swanston DN, Ziemer RR, Janda RJ. 1995. Rate and mechanisms of progressive hillslope failure in the Redwood Creek basin, northwestern California. In *Geomorphic Processes and Aquatic Habitat in the Redwood Creek Basin, Northwestern California*. E1–E16 US Geological Survey Professional Paper, No. 1454.
Thompson SK. 1992. *Sampling*. John Wiley: New York.
US Environmental Protection Agency. 1999. *Total maximum daily loads for sediment, Redwood Creek, CA*.